Charged–Higgs effects in a new $B \to D\tau\nu_\tau$ differential decay distribution

Ulrich Nierste, Stéphanie Trine, and Susanne Westhoff

Institut für Theoretische Teilchenphysik
Karlsruhe Institute of Technology, 76128 Karlsruhe, Germany

We show that the decay mode $B \to D\tau\nu_\tau$ is competitive with and complementary to $B \to \tau\nu_\tau$ in the search for charged–Higgs effects. Updating the relevant formfactors, we find that the differential distribution in the decay chain $\bar{B} \to D\bar{\nu}_\tau\tau^-[\to \pi^-\nu_\tau]$ excellently discriminates between Standard–Model and charged–Higgs contributions. By measuring the D and π^- energies and the angle between the D and π^- tracks one can determine the effective charged–Higgs coupling including a possible CP–violating phase.

1. Introduction. The B factories BaBar and BELLE have accumulated enough statistics to probe extensions of the Higgs sector of the Standard Model. Notably, the decay $B^+ \to \tau^+\nu_\tau$ allows us to place first constraints on the parameters $\tan\beta$ and M_{H^+} of the two–Higgs–doublet model (2HDM) of type II [1]. Here $\tan\beta$ is the ratio of the two Higgs vacuum expectation values and M_{H^+} is the mass of the physical charged Higgs boson H^+ in the model. Since the couplings of H^+ to b's and τ's grow with $\tan\beta$, $B^+ \to \tau^+\nu_\tau$ probes large values of $\tan\beta$. At tree–level the Higgs sector of the Minimal Supersymmetric Standard Model (MSSM) coincides with the type–II 2HDM. The coupling of H^+ to fermions can be modified by a factor of order one due to $\tan\beta$–enhanced radiative corrections [3, 4], yet this introduces only a few additional supersymmetric parameters and the access to the Higgs sector is not obfuscated like in many other modes, such as $b \to s\gamma$. This explains the great theoretical interest in the experimental ranges for $\mathcal{B}(B^+ \to \tau^+\nu_\tau)$ [2].

The decay $B \to D\tau\nu_\tau$ provides an alternative route to charged–Higgs effects [5, 6]. As we will show in the following, this mode is not only competitive with $B^+ \to \tau^+\nu_\tau$, it also opens the door to a potential CP–violating phase in the Yukawa couplings of the H^+ to b and τ. $B \to D\tau\nu_\tau$ compares to $B \to \tau\nu_\tau$ as follows:

i) $\mathcal{B}(B \to D\tau\nu_\tau)$ exceeds $\mathcal{B}(B \to \tau\nu_\tau)$ by roughly a factor of 50 in the Standard Model.

ii) $B \to D\tau\nu_\tau$ involves the well–known element V_{cb} of the Cabibbo–Kobayashi–Maskawa (CKM) matrix. The uncertainty on $|V_{ub}|$ entering $B \to \tau\nu_\tau$ is much larger.

iii) $\mathcal{B}(B \to \tau\nu_\tau)$ is proportional to two powers of the B decay constant f_B, which must be obtained with non–perturbative methods. Current lattice gauge theory computations are struggling with chiral logarithms and f_B^2 can only be determined with an uncertainty of 30% or more [7]. $B \to D\tau\nu_\tau$ involves two formfactors, one of which can be measured in $B \to D\ell\nu_\ell$ ($\ell = e, \mu$) decays [8, 9]. The other one is tightly constrained by Heavy Quark Effective Theory (HQET) [10, 11], so that hadronic uncertainties can be reduced to less than 10% once the measurement of $B \to D\ell\nu_\ell$ is improved.

iv) Unlike $B \to \tau\nu_\tau$ the three–body decay $B \to D\tau\nu_\tau$ permits the study of decay distributions which discriminate between W^+ and H^+ exchange [12–14].

v) The Standard Model (SM) contribution to $B \to \tau\nu_\tau$ is helicity–suppressed, so that the sensitivity of $\mathcal{B}(B \to \tau\nu_\tau)$ to H^+ is enhanced. For $B \to D\tau\nu_\tau$ a similar effect only occurs near the kinematic endpoint, where the D moves slowly in the B rest frame [12]: While the transversely polarized W^+ contribution suffers from a P–wave suppression, the virtual H^+ recoils against the D meson in an unsuppressed S–wave.

Items iv) and v) strongly suggest to study differential decay distributions in $B \to D\tau\nu_\tau$. The τ in the final state poses an experimental challenge, because it does not travel far enough for a displaced vertex and its decay involves at least one more neutrino. In particular, the τ polarization, known as a charged-Higgs analyzer, is not directly accessible to experiment [5]. The most straightforward way to deal with this is to consider the full decay chain down to the detectable particles stemming from the τ. We have studied the decays $\tau^- \to \pi^-\nu_\tau$, $\tau^- \to \rho^-\nu_\tau$, and $\tau^- \to \ell^-\bar{\nu}_\ell\nu_\tau$ and assessed the sensitivity of the decay distributions to H^+ effects. We find that the decay chain $\bar{B} \to D\bar{\nu}_\tau\tau^-[\to \pi^-\nu_\tau]$ discriminates between W^+ and H^+ exchange in an excellent way. In this Letter we present the results for the differential decay rate as a function of the D and π^- energies and the angle between the D and π^- three–momenta for this decay chain. Our result greatly facilitates the determination of the effective coupling g_S governing H^+ exchange, including a potential complex phase. A conventional analysis combining Monte Carlo simulations of $\bar{B} \to D\bar{\nu}_\tau\tau^-$ and $\tau^- \to \pi^-\nu_\tau$ decays would be very cumbersome, because the $B \to D\tau\nu_\tau$ differential distributions strongly depend on the a–priori unknown value of g_S.

2. $B \to D$ formfactors. The effective hamiltonian describing $B \to (D)\tau\nu_\tau$ transitions mediated by W^+ or H^+ reads (with $q = u\,(c)$)

$$\begin{aligned} H_{\text{eff}} = \frac{G_F}{\sqrt{2}} V_{qb} \, \{ \, [\overline{q}\gamma^\mu(1-\gamma_5)b] \; [\overline{\tau}\gamma_\mu(1-\gamma_5)\nu_\tau] \\ - \frac{\overline{m}_b m_\tau}{m_B^2} \, \overline{q}\,[g_S + g_P\gamma_5]\,b\,[\overline{\tau}(1-\gamma_5)\nu_\tau] \, \} + \text{h.c.} \end{aligned} \tag{1}$$

The effective coupling constant g_P only enters the $B \to \tau\nu_\tau$ decay, while $B \to D\tau\nu_\tau$ is only sensitive to g_S. The B^+ meson mass m_B is introduced in Eq. (1), so that $\mathcal{B}(B \to \tau\nu_\tau)$ vanishes for $g_P = 1$. The above operators as well as $\overline{m}_b$ are defined in the $\overline{\text{MS}}$ scheme. In the MSSM, which is our main focus, one has $g_S = g_P$.

The analysis of $B \to D\tau\nu_\tau$ requires the knowledge of the formfactors F_V and F_S which parametrize the vector and scalar current matrix elements:

$$\langle D(p_D)|\bar{c}\gamma^\mu b|\bar{B}(p_B)\rangle = F_V(q^2)\left[p_B^\mu + p_D^\mu - m_B^2\frac{1-r^2}{q^2}q^\mu\right] + F_S(q^2)\, m_B^2\frac{1-r^2}{q^2}q^\mu\,,$$
$$\langle D(p_D)|\bar{c}b|\bar{B}(p_B)\rangle = \frac{m_B^2\,(1-r^2)}{\overline{m}_b - \overline{m}_c}F_S(q^2)\,, \qquad (2)$$

where p_B and p_D denote the meson four–momenta, $q = p_B - p_D$, and $r = m_D/m_B$. It is convenient to introduce the normalized formfactors $V_1 \equiv F_V\,2\sqrt{r}/(1+r)$ and $S_1 \equiv F_S(1+r)/(2\sqrt{r})$, as well as the kinematic variable $w \equiv (1+r^2-q^2/m_B^2)/2r$. In the limit of infinitely heavy quark masses $m_Q = m_b,\, m_c$ (which are properly infrared–subtracted pole masses), both $V_1(w)$ and $S_1(w)$ reduce to the universal Isgur–Wise function $\xi(w)$, normalized to $\xi(1) = 1$. At the kinematic endpoint $w = 1$, corrections to this limit read

$$V_1(1) = \eta_v - \frac{1-r}{1+r}\left(\delta_{\text{rad}} + \delta_{1/m_Q}\right), \quad S_1(1) = \eta_v\,, \qquad (3)$$

up to $\mathcal{O}(\alpha_s^2, 1/m_Q^2)$. Here η_v denotes radiative corrections in the limit of equal heavy meson masses, and δ_{rad} (δ_{1/m_Q}) are the first order radiative ($1/m_Q$) corrections to the function ξ_- defined in [10]. The δ_{1/m_Q} term depends on the subleading function $\xi_3(w=1) = \bar{\Lambda}\eta(w=1)$ and on the HQET parameter $\bar{\Lambda}$. We take $\bar{\Lambda} = 0.5 \pm 0.1$ GeV, $\eta(1) = 0.6 \pm 0.2$ [15], η_v and δ_{rad} to $\mathcal{O}(\alpha_s)$ from Ref. [16], and add a 5% error to the formfactors at $w = 1$ to account for higher order corrections. We obtain $V_1(1) = 1.05 \pm 0.08$ and $S_1(1) = 1.02 \pm 0.05$.

The semileptonic decay into light leptons $B \to D\ell\nu_\ell$ depends solely on the vector formfactor $V_1(w)$. The measured quantity $|V_{cb}|V_1(w)$ was fitted by the BELLE collaboration [8] to a two–parameter ansatz $V_1(w, V_1(1), \rho_1^2)$ derived from dispersion relations and heavy quark spin symmetry [11]. The fitted curve, however, suffers from large statistical and systematic uncertainties near $w = 1$. We thus take $V_1(1)$ from HQET instead, use $|V_{cb}| = (4.17 \pm 0.07)\%$ from inclusive semileptonic B decays [17], and only fix the formfactor at large recoil $w = 1.45$ from the data, including the dominant systematic errors in a conservative way: $|V_{cb}|V_1(1.45) = (2.63 \pm 0.51)\%$. The formfactor over the whole kinematic range is then obtained using a two–parameter description $F_V(w, a_0^V, a_1^V)$, which uses a conformal mapping $w \to z(w)$ resulting in an essentially linear dependence of F_V on z [18]. This linearity in $z(w)$ is confirmed by the fact that fitting the $B \to D\ell\nu_\ell$ data with both F_V parametrizations without further theoretical constraints essentially gives the same result (see Fig. 1). The sets of parameters corresponding to the minimal and maximal formfactors satisfying the HQET constraint at $w = 1$ are displayed in Tab. I for both parametrizations $V_1(w, V_1(1), \rho_1^2)$ and $F_V(w, a_0^V, a_1^V)$. They delimit the gray area in Fig. 1. The HFAG [9] treats systematic errors in a different way and (including CLEO and ALEPH data) finds smaller uncertainties at large recoil.

Similarly, the scalar formfactor $F_S(w, a_0^S, a_1^S)$ is constrained by HQET at $w = 1$, while its value at large recoil is fixed from the relation $F_S(q^2=0) = F_V(q^2=0)$. The resulting parameters are displayed in the third line of Tab. I.

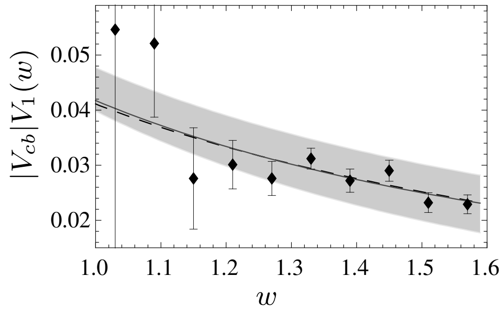

FIG. 1: Vector formfactor $V_1(w)$. Dots: exp. data [8] with stat. errors only. Dashed: fit to parametrization in [11]. Plain: fit to linear parametrization in [18]. Gray band: formfactor with HQET constraint at $w = 1$; systematic errors dominate at large recoil.

Parameters	minimal $F(w)$	maximal $F(w)$	central $F(w)$
$\{V_1(1), \rho_1^2\}$	$\{0.97, 1.47\}$	$\{1.13, 1.06\}$	$\{1.05, 1.24\}$
$\{a_0^V, a_1^V\}[10^{-4}]$	$\{2.30, -14\}$	$\{3.01, -5\}$	$\{2.66, -9\}$
$\{a_0^S, a_1^S\}[10^{-3}]$	$\{3.96, -26\}$	$\{5.05, -7\}$	$\{4.52, -16\}$

TABLE I: Parameters $\{V_1(1), \rho_1^2\}$ for F_V [11] and $\{a_0^{V,S}, a_1^{V,S}\}$ for $F_{V,S}$ (see [18], $Q^2 = 0$, $\eta = 2$, subthreshold poles: $m(1^-) = 6.337,\ 6.899,\ 7.012$ GeV and $m(0^+) = 6.700,\ 7.108$ GeV [19]).

3. Charged–Higgs effects. The MSSM is a well–motivated new–physics scenario in which charged scalar current interactions occur at tree–level. Resumming the dominant $\tan\beta$-enhanced loop corrections to all orders, the couplings $g_{S,P}$ in Eq. (1) specify to [6, 20]

$$g_S = g_P = \frac{m_B^2}{M_{H^+}^2}\,\frac{\tan^2\beta}{(1+\widetilde{\epsilon}_0\,\tan\beta)(1+\epsilon_\tau\,\tan\beta)}\,. \qquad (4)$$

This particular form holds in MSSM scenarios with Minimal Flavor Violation (MFV). The loop factor $\widetilde{\epsilon}_0$ arises from the quark Yukawa sector and depends on ratios of superparticle masses, resulting in a sizable non–decoupling effect $\widetilde{\epsilon}_0\tan\beta = \mathcal{O}(1)$ for $\tan\beta = \mathcal{O}(50)$. ϵ_τ comprises the corresponding effect for the τ lepton. $\widetilde{\epsilon}_0$ and ϵ_τ can receive sizable complex phases from the Higgsino mass parameter μ, if first–generation sfermions are sufficiently heavy to soften the impact of the bounds on electric dipole moments on $\arg\mu$. Beyond MFV also phases from squark mass matrices will easily render g_S complex. It is therefore mandatory to constrain – and eventually measure – both magnitude and phase of g_S. The type–II 2HDM is recovered setting $\widetilde{\epsilon}_0 = \epsilon_\tau = 0$.

The $B \to D\tau\nu_\tau$ branching ratio has recently been measured by the BaBar collaboration [21]:

$$R^{\text{exp}} \equiv \frac{\mathcal{B}(B\to D\tau\nu_\tau)}{\mathcal{B}(B\to D\ell\nu_\ell)} = (41.6 \pm 11.7 \pm 5.2)\%\,. \qquad (5)$$

The normalization to $\mathcal{B}(B \to D\ell\nu_\ell)$ reduces the dependence on the vector formfactor F_V and thus tames the main theoretical uncertainties. In the presence of charged–Higgs contributions, the theoretical ratio is approximated to 1% by

$$R^{\rm th} = \frac{1.126 + 0.037\, r_V + r_0^2\,(1.544 + 0.082\, r_S + N_{H^+})}{10 - 0.95\, r_V}\,,$$
$$\begin{aligned} N_{H^+} &= -\, r_{cb}\, Re[g_S]\,(1.038 + 0.076\, r_S) \\ &\quad + r_{cb}^2\, |g_S|^2\,(0.186 + 0.017\, r_S), \end{aligned} \qquad (6)$$

with $r_V = (a_1^V/a_0^V)/(-3.4)$, $r_S = (a_1^S/a_0^S)/(-3.5)$, $r_0 = (a_0^S/a_0^V)/17$, and $r_{cb} = 0.8/(1 - \overline{m}_c/\overline{m}_b)$. The dependence on the slope parameters $a_1^{V,S}$ appears to be quite mild. In Fig. 2 we compare $R^{\rm th}$ to the one–sigma measurement for positive g_S. We also display the theoretical prediction without experimental uncertainties on the formfactors at large recoil to emphasize the importance of a better experimental knowledge of the $B \to D\ell\nu_\ell$ modes. Taking F_V from the HFAG [9], the error band is close to the dark gray band.

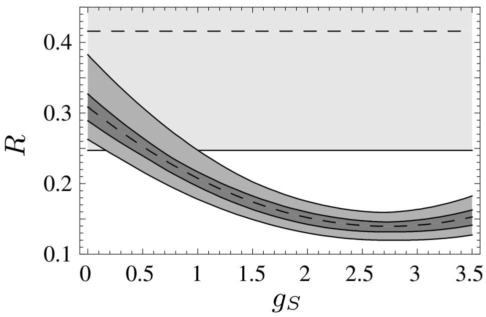

FIG. 2: $R \equiv \mathcal{B}(B \to D\tau\nu_\tau)/\mathcal{B}(B \to D\ell\nu_\ell)$ as a function of g_S. Light gray band: $R^{\rm exp}$, see (5) [21]. Gray band: $R^{\rm th}$, see (6). Dark gray band: $R^{\rm th}$ without experimental systematic errors on the formfactors. SM: $R^{\rm th}(g_S = 0) = 0.31\,^{+0.07}_{-0.05}$ (gray) [± 0.02 (dark gray)].

The $B \to D\tau\nu_\tau$ branching fraction is promising to discover – or constrain – charged–Higgs effects, but not to measure g_S with good precision, as the dependence in Fig. 2 is too flat. The differential distribution in the decay chain $\bar{B} \to D\bar{\nu}_\tau\tau^-[\to \pi^-\nu_\tau]$ is better suited for that purpose. The experimentally accessible quantities are the energies E_D and E_π of the D and π^- mesons, respectively, and the angle θ between the three–momenta $\vec{p}_D$ and $\vec{p}_\pi$. We define these quantities in the B rest frame. We integrate over the phase space of the two unobserved neutrinos in the final state. Our formulae contain the full spin correlation between the production and decay of the τ, which is important to discriminate between SM and charged–Higgs contributions. This approach further facilitates the rejection of backgrounds from neutral particles escaping detection, as in $\bar{B} \to DD^-[\to \pi^-\pi^0]$ with an undetected π^0: If the mass of the undetected particle is m, this background can be suppressed by cuts excluding the region around

$$\cos\theta = \frac{(m_B - E_D - E_\pi)^2 - 2(E_D^2 - m_D^2) - m^2}{2(E_D^2 - m_D^2)}\,. \qquad (7)$$

We obtain the differential distribution

$$\frac{d\Gamma(\bar{B} \to D\bar{\nu}_\tau\tau^-[\to \pi^-\nu_\tau])}{dE_D\, dE_\pi\, d\cos\theta} = G_F^4 f_\pi^2 |V_{ud}|^2 |V_{cb}|^2 \tau_\tau \qquad (8)$$
$$\times \left[C_W(F_V, F_S) - C_{WH}(F_V, F_S)\, Re[g_S] + C_H(F_S)|g_S|^2\right]$$

with formfactor–dependent functions of E_D, E_π, and $\cos\theta$ for the SM (C_W), interference (C_{WH}), and Higgs (C_H) contributions, given as follows for vanishing m_π (this approximation, which is good to 1%, is not used in our numerical analysis),

$$\begin{aligned} C_W &= \kappa \frac{m_\tau^4}{2} \frac{l^2}{p_\pi \cdot l} \left\{ P^2(b-1) + (P\cdot l)^2 \frac{2b}{l^2} + \right. \\ &\quad \left. \left[\frac{l^2 (P\cdot p_\pi)^2}{(p_\pi \cdot l)^2} - \frac{2(P\cdot l)(P\cdot p_\pi)}{p_\pi \cdot l} \right] (3b-1) \right\}, \\ C_{WH} &= 2\kappa\, m_\tau^4\, \frac{(1-r^2)F_S}{1 - \overline{m}_c/\overline{m}_b}\, b \left[P\cdot l - \frac{l^2 P\cdot p_\pi}{p_\pi \cdot l} \right], \\ C_H &= \kappa\, m_\tau^6 \frac{(1-r^2)^2 F_S^2}{(1 - \overline{m}_c/\overline{m}_b)^2} \left(1 - \frac{m_\tau^2}{2\, p_\pi \cdot l}\right), \end{aligned} \qquad (9)$$

where $\overline{m}_c$ and $\overline{m}_b$ must be evaluated at the same scale so that $\overline{m}_c/\overline{m}_b = 0.20 \pm 0.02$ [22], and

$$\begin{aligned} P &= F_V(p_B + p_D) - (F_V - F_S) \frac{m_B^2(1-r^2)}{q^2}(p_B - p_D)\,, \\ \kappa &= \frac{E_\pi \sqrt{E_D^2 - m_D^2}}{128\,\pi^4\, m_B m_\tau}\,, \quad b = \frac{m_\tau^2}{p_\pi \cdot l}\left(1 - \frac{m_\tau^2}{2\, p_\pi \cdot l}\right), \\ l &= p_B - p_D - p_\pi\,, \quad q^2 = (p_B - p_D)^2. \end{aligned} \qquad (10)$$

The dot products appearing in Eqs. (9) and (10) are related to the energies, momenta, and the angle θ measured in the B rest frame as $p_B \cdot l = m_B(m_B - E_D - E_\pi)$, $p_D \cdot l = E_D(m_B - E_D - E_\pi) + |\vec{p}_D|^2 + |\vec{p}_D| E_\pi \cos\theta$, $p_\pi \cdot l = E_\pi(m_B - E_D) + |\vec{p}_D| E_\pi \cos\theta$, and $p_B \cdot p_D = m_B E_D$. Further $\tau_\tau = (290.6 \pm 1.0) \times 10^{-15} s$ is the τ lepton lifetime, $f_\pi = (130.7 \pm 0.1 \pm 0.36)$ MeV the pion decay constant, and the CKM matrix elements are $|V_{ud}| = 0.97377 \pm 0.00027$ and $|V_{cb}| = (41.7 \pm 0.7) \times 10^{-3}$, the latter being well determined from inclusive semileptonic B decays [17]. Remarkably, one can probe a CP–violating phase of g_S by exploiting the shape of the distribution in Eq. (8), which is not possible from the branching fraction of either $B \to D\tau\nu_\tau$ or $B \to \tau\nu_\tau$.

We show the differential decay distribution including charged–Higgs effects in comparison with the SM for the meson energies $E_D = 2$ GeV and $E_\pi = 1$ GeV, so that the whole range of $\cos\theta$ is kinematically accessible. In this particular region of phase space the SM rate is strongly suppressed for $\cos\theta = -1$. For a large scalar coupling $g_S = 2$ (Fig. 3, left), the Higgs contribution dominates the rate at this point (dark gray band), such that we can clearly distinguish it from the SM (light gray band). The experimental information from $\mathcal{B}(B \to \tau\nu_\tau)$ constrains $|1 - g_P|$. For real g_P this permits a range near $g_P = 0$ and another range around $g_P = 2$. In the MSSM situation with $g_P = g_S$, the case $g_S = 2$ therefore is in agreement with $B \to \tau\nu_\tau$, but can be confirmed

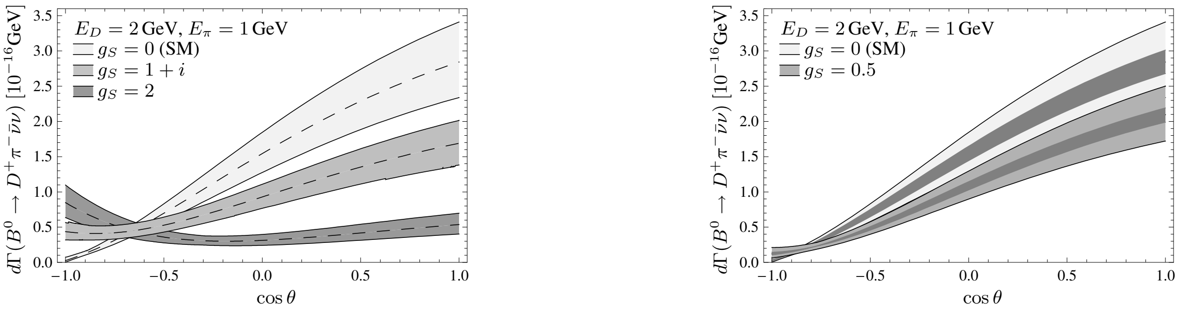

FIG. 3: $\bar{B}^0 \to D^+\bar{\nu}_\tau\tau^-[\to \pi^-\nu_\tau]$ angular distribution for $E_D = 2\,\mathrm{GeV}$ and $E_\pi = 1\,\mathrm{GeV}$. Left: $g_S = 0, 1+i, 2$. Right: $g_S = 0, 0.5$ (dark gray: without uncertainties in $F_V(w)$ and V_{cb}, errors from $S_1(1)$ and $\overline{m}_c/\overline{m}_b$).

or ruled out by measuring our distribution. The discrimination potential for the phase of g_S shows up in the light gray band: It corresponds to a complex $g_S = 1 + i$, which yields the same $\mathcal{B}(B \to \tau\nu_\tau)$ as $g_S = 0, 2$. The $B \to D\tau\nu_\tau$ branching ratio alone may also help to distinguish between these solutions, depending on the future experimental value of $\mathcal{B}(B \to D\tau\nu_\tau)$, see Fig. 2. For general g_S values, a fit to the differential distribution in Eq. (8) would excellently quantify charged–Higgs effects, especially once better experimental information is available, as we illustrate in Fig. 3 (right–hand side) for $g_S = 0.5$ and fixed D and π^- energies.

4. Conclusions. We have studied charged–Higgs effects in a differential distribution of the decay chain $\bar{B} \to D\bar{\nu}_\tau\tau^-[\to \pi^-\nu_\tau]$, which has the following advantages over the branching fractions $\mathcal{B}(B \to \tau\nu_\tau)$ and $\mathcal{B}(B \to D\tau\nu_\tau)$:

i) The Higgs coupling constant g_S can be determined from the *shape* of the distribution in sensitive phase space regions. This analysis should be possible with current B factory data.

ii) The dependence on both $|g_S|$ and $\mathrm{Re}\,[g_S]$ allows to quantify a possible CP–violating phase. Since our decay distribution is a CP–conserving quantity, the phase of g_S is determined with a two–fold ambiguity. In the MSSM such a phase stems from the μ parameter or the soft breaking terms and enters through the $\tan\beta$–enhanced loop factors $\widetilde{\epsilon}_0, \epsilon_\tau$. Collider studies of this phase involve smaller loop factors and require the measurements of tiny asymmetries [23].

The main uncertainties stem from the formfactors. One can gain a much better accuracy with better data on the vector formfactor F_V. The recent $B \to D\ell\nu_\ell$ measurement by BaBar [24] furnishes promising data for a new fit.

Within the MSSM, one will be able to place new constraints on the $\tan\beta - M_{H^+}$ plane, once our results are confronted with actual data from the B factories. If $\tan\beta/M_{H^+}$ is indeed large, there is a fair chance to reveal charged–Higgs effects ahead of the LHC.

Acknowledgments: The authors acknowledge helpful discussions with Richard Hill and Michael Feindt. This work is supported in part by the DFG grant No. NI 1105/1–1, by the DFG–SFB/TR9, and by the EU Contract No. MRTN-CT-2006-035482, "FLAVIAnet".

[1] W. Hou, Phys. Rev. D **48**, 2342 (1993).
[2] BELLE Collaboration, Phys. Rev. Lett. **97**, 251802 (2006); BABAR Collaboration, Phys. Rev. D **76**, 052002 (2007).
[3] L. Hall, R. Rattazzi and U. Sarid, Phys. Rev. D **50**, 7048 (1994); T. Blazek, S. Raby and S. Pokorski, Phys. Rev. D **52**, 4151 (1995). M. Carena *et al.*, Nucl. Phys. B **577**, 88 (2000).
[4] A. Akeroyd and S. Recksiegel, J. Phys. G **29**, 2311 (2003).
[5] M. Tanaka, Z. Phys. C **67**, 321 (1995).
[6] H. Itoh, S. Komine and Y. Okada, Prog. Theor. Phys. **114**, 179 (2005).
[7] M. Della Morte, PoS LAT2007, 8.
[8] BELLE Collaboration, Phys. Lett. B **526**, 258 (2002).
[9] Heavy Flavor Averaging Group, [0704.3575][hep-ex].
[10] M. Neubert, Phys. Rept. **245**, 259 (1994).
[11] I. Caprini, L. Lellouch and M. Neubert, Nucl. Phys. B **530**, 153 (1998).
[12] B. Grzadkowski and W. Hou, Phys. Lett. B **283**, 427 (1992).
[13] K. Kiers and A. Soni, Phys. Rev. D **56**, 5786 (1997).
[14] T. Miki, T. Miura and M. Tanaka, [hep-ph/0210051].
[15] Z. Ligeti, Y. Nir and M. Neubert, Phys. Rev. D **49**, 1302 (1994).
[16] M. Neubert, Phys. Rev. D **46**, 2212 (1992).
[17] W.-M. Yao *et al.* [Particle Data Group], J. Phys. G **33**, 1 (2006).
[18] R. Hill, [hep-ph/0606023].
[19] E. Eichten and C. Quigg, Phys. Rev. D **49**, 5845 (1994).
[20] A. Buras *et al.*, Nucl. Phys. B **659**, 3 (2003).
[21] BABAR Collaboration, Phys. Rev. Lett. **100**, 021801 (2008).
[22] K. Chetyrkin, J. Kühn and M. Steinhauser, Comput. Phys. Commun. **133**, 43 (2000). Input values: J. Kühn, M. Steinhauser and C. Sturm, Nucl. Phys. B **778**, 192 (2007).
[23] E. Accomando *et al.*, [hep-ph/0608079], and references therein.
[24] BABAR Collaboration, [0708.1738][hep-ex].